

Latest results on exotic hadrons from CMS

Jingqing Zhang^{a,*} on behalf of the CMS Collaboration

*^aSchool of Physics and Technology, Nanjing Normal University,
No.1 Wenyuan Road, Nanjing, China*

E-mail: jingqing.zhang@njnu.edu.cn

The exotic hadrons which have quark configuration different to mesons ($q\bar{q}$) and baryons (qqq) are allowed in QCD theory. Search and study exotic hadrons is helpful to deepen our understanding of the QCD theory. In this report, recent results on exotic hadrons from the CMS experiment are presented.

*21st Conference on Flavor Physics and CP Violation (FPCP 2023)
29 May - 2 June 2023
Lyon, France*

*Speaker

1. Introduction

The Quantum Chromodynamics (QCD) is the theory to describe the strong interaction in the standard model of the particle physics. Its success has been proved in many experimental results. Within the QCD framework, hadrons have the quark configuration of $q\bar{q}$ (meson) or qqq (baryon). Exotic hadrons, which are beyond the conventional $q\bar{q}$ and qqq configuration, are allowed in the QCD theory. Search and study exotic hadrons will help deepen our understanding of the QCD theory.

The CMS experiment [1] at the LHC has performed many studies in exotic hadron search and study. This contribution will introduce the latest results on exotic hadrons from the CMS experiment, including the first observation of $B_s^0 \rightarrow X(3872)\phi$ decay [2], and observation of new structure in $J/\psi J/\psi$ invariant mass spectrum [3].

2. Observation of the $B_s^0 \rightarrow X(3872)\phi$ Decay

The $X(3872)$ was first observed by Belle Collaboration in the $B^+ \rightarrow J/\psi\pi^+\pi^-K^+$ decay in 2003 [4]. Its near-threshold mass and small natural width suggest that it is unlikely a usual charmonium resonance, and its nature is still unclear.

The CMS Collaboration observed the $B_s^0 \rightarrow X(3872)\phi$ decay for the first time, using the proton-proton collision data recored by the CMS detector in 2016–2018 at $\sqrt{s} = 13$ TeV, corresponding to an integrated luminosity of 140 fb^{-1} [2]. The signal channel $B_s^0 \rightarrow X(3872)\phi$ is reconstructed using the subsequent decays $X(3872) \rightarrow J/\psi\pi^+\pi^-$, $J/\psi \rightarrow \mu^+\mu^-$, and $\phi \rightarrow K^+K^-$. The branching fraction of the signal channel is measured with respect to the reference channel $B_s^0 \rightarrow \psi(2S)\phi$ as:

$$\begin{aligned} R &= \frac{\mathcal{B}[B_s^0 \rightarrow X(3872)\phi]\mathcal{B}[X(3872) \rightarrow J/\psi\pi^+\pi^-]}{\mathcal{B}[B_s^0 \rightarrow \psi(2S)\phi]\mathcal{B}[\psi(2S) \rightarrow J/\psi\pi^+\pi^-]} \\ &= \frac{N[B_s^0 \rightarrow X(3872)\phi]}{N[B_s^0 \rightarrow \psi(2S)\phi]} \frac{\epsilon_{B_s^0 \rightarrow \psi(2S)\phi}}{\epsilon_{B_s^0 \rightarrow X(3872)\phi}}, \end{aligned} \quad (1)$$

where N stands for the measured number of signal events in data, and ϵ stands for the efficiency.

Figure 1 shows the observed $J/\psi\pi^+\pi^-$ (left) and K^+K^- (right) invariant mass distributions for the $B_s^0 \rightarrow \psi(2S)\phi$ candidates, where the red lines are projections of a 2D fit to extract $\psi(2S)\phi$ signal yields. The same distributions for $B_s^0 \rightarrow X(3872)\phi$ candidates are shown in Fig. 2, where contribution from $X(3872)\phi$ component is observed with a significance over 6 standard deviations (σ).

Figure 3 shows the background-subtracted $\psi(2S)\phi$ (left) and $X(3872)\phi$ (right) invariant mass distributions using sPlot method [5]. The non- B_s^0 background contribution for $\psi(2S)\phi$ and $X(3872)\phi$ is determined to be 0.5% and 1.7%, respectively. The ratio R of branching fractions is measured to be $R = [2.21 \pm 0.29(\text{stat}) \pm 0.17(\text{syst})]\%$.

3. Observation of new structure in the $J/\psi J/\psi$ invariant mass spectrum

The $X(3872)$ and many other exotic candidates contain two heavy quark ($c\bar{c}$). An analogue to heavy quarkonia would be fully heavy tetraquarks. A full heavy exotic candidate is the $X(6900)$

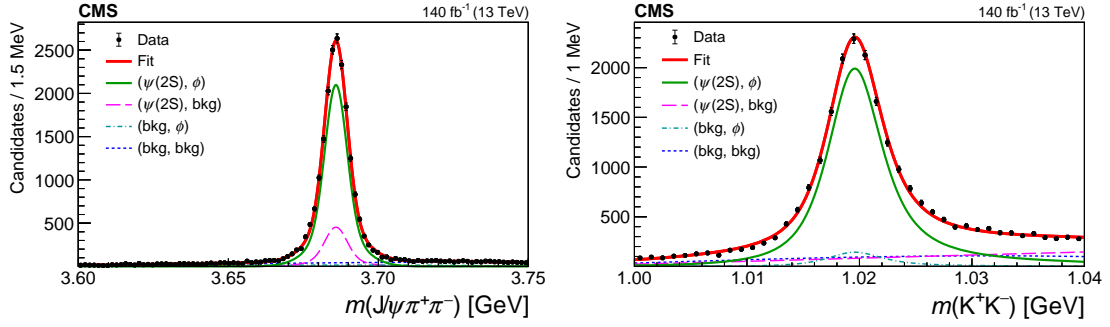


Figure 1: The observed $J/\psi\pi^+\pi^-$ (left) and K^+K^- (right) invariant mass distributions for the $B_s^0 \rightarrow \psi(2S)\phi$ candidates are shown by points, with the vertical bars representing the statistical uncertainties [2]. The projections of the 2D fit and its various components are shown by the lines.

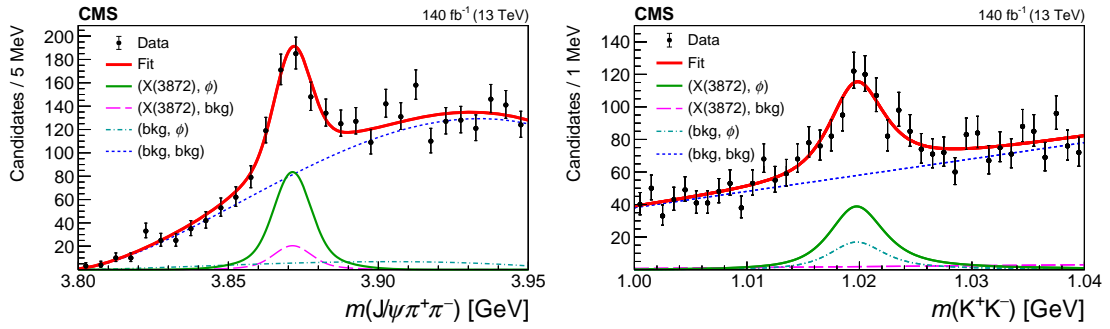


Figure 2: The observed $J/\psi\pi^+\pi^-$ (left) and K^+K^- (right) invariant mass distributions for the $B_s^0 \rightarrow X(3872)\phi$ candidates are shown by points, with the vertical bars representing the statistical uncertainties [2]. The projections of the 2D fit and its various components are shown by the lines.

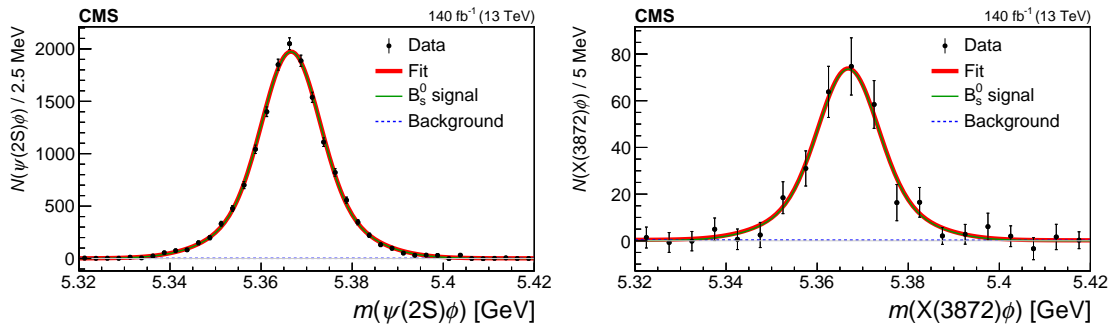


Figure 3: Background-subtracted $\psi(2S)\phi$ (left) and $X(3872)\phi$ (right) invariant mass distributions obtained by sPlot weighting [2]. The result of each fit and its components are shown by lines.

decaying into $J/\psi J/\psi$ reported by the LHCb Collaboration first [6], and confirmed by both ATLAS [7] and CMS [3].

The CMS experiment performed a study of the near-threshold invariant mass distribution of $J/\psi J/\psi$, using a data sample corresponding to an integrated luminosity of 135 fb^{-1} at a center-of-mass energy of 13 TeV [3]. In the analysis, the two J/ψ candidates are reconstructed using their $\mu^+\mu^-$ mode.

The observed $J/\psi J/\psi$ invariant mass spectrum is shown in Fig. 4. To describe the data,

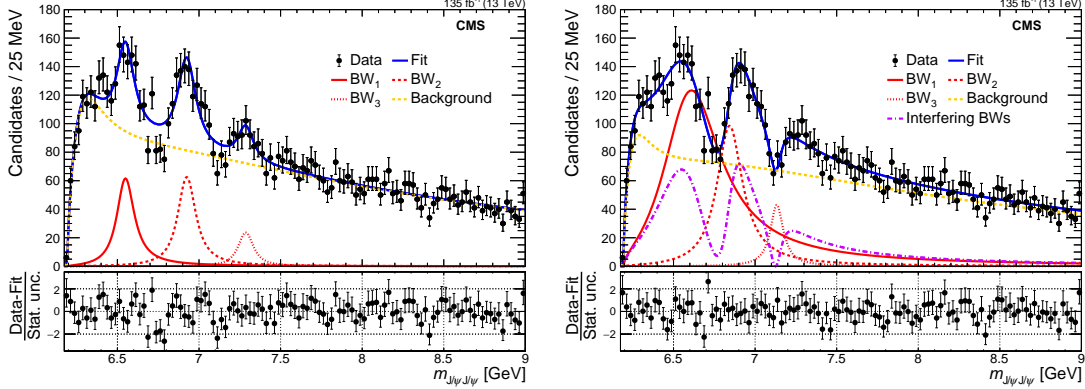


Figure 4: The $J/\psi J/\psi$ invariant mass spectrum in the range up to 9 GeV, with fits consisting of three signal functions ($BW_1/X(6600)$, $BW_2/X(6900)$, and $BW_3/X(7300)$) and a background model (NRSPS+NRDPS+ BW_0) [3]. The left plot shows the fit without interference, while the right plot shows the fit that includes interference, where the "Interfering BWs" refers to the total contribution of all the interfering amplitudes, and their cross-terms. The lower portion of the plots shows the pulls, i.e., the number of standard deviations (statistical uncertainties only) that the binned data differ from the fit.

three signal structures, $X(6600)$, $X(6900)$, and $X(7300)$ are needed, which are described by S-wave Breit-Wigner functions. The background contribution includes in non-resonant single parton scattering (NRSPS), double parton scattering (DPS), and an *ad-hoc* component, a near-threshold Breit-Wigner(BW_0). Figure 4 (left) shows the fit without considering possible interference effects between Breit-Wigner structures. The statistical significance of the signal structures are 6.5σ , 9.4σ , and 4.1σ . The measured mass, width, and yields of each states are shown in Table 1. To improve the description of the invariant mass distribution, a model including interference between the three signal structures is performed, and the fit projection is shown in Fig. 4 (right). This fit improves the signal-region ($< 7.8 \text{ GeV}$) χ^2 probability from 9% to 65%. The measured mass and width of each state in the interference model are shown in Table 1. The mass and width of the $X(6900)$ are consistent with values reported by LHCb [6] and the recent measurement from ATLAS [7] within 2σ .

4. Summary

In summary, recent results on exotic hadrons from the CMS experiment are presented. The results include in the first observation of the $B_s^0 \rightarrow X(3872)\phi$ decay [2], and the $X(6600) \rightarrow J/\psi J/\psi$ decay [3]. The first evidence of the $X(7300)$ and the confirmation of the $X(6900)$ in $J/\psi J/\psi$ invariant mass distribution [3] are also presented.

Table 1: Summary of the fit results for the $J/\psi J/\psi$ invariant mass distribution. The mass m and natural width Γ for both the no-interference model and the interference model, and the signal yields N for the no-interference model, are given for the three signal structures. The dual uncertainties are the statistical followed by the systematic components, and single uncertainties are only statistical.

		BW ₁	BW ₂	BW ₃
No-interference	m [MeV]	$6552 \pm 10 \pm 12$	$6927 \pm 9 \pm 4$	$7287^{+20}_{-18} \pm 5$
	Γ [MeV]	$124^{+32}_{-26} \pm 33$	$122^{+24}_{-21} \pm 18$	$95^{+59}_{-40} \pm 19$
	N	470^{+120}_{-110}	492^{+78}_{-73}	156^{+64}_{-51}
Interference	m [MeV]	6638^{+43+16}_{-38-31}	6847^{+44+48}_{-28-20}	7134^{+48+41}_{-25-15}
	Γ [MeV]	$440^{+230+110}_{-200-240}$	191^{+66+25}_{-49-17}	97^{+40+29}_{-29-26}

References

- [1] CMS Collaboration, The CMS Experiment at the CERN LHC, JINST **3** (2008), S08004 doi:10.1088/1748-0221/3/08/S08004.
- [2] CMS Collaboration, Observation of the $B_s^0 \rightarrow X(3872)\phi$ decay, Phys. Rev. Lett. **125** (2020) no.15, 152001 doi:10.1103/PhysRevLett.125.152001 [arXiv:2005.04764 [hep-ex]].
- [3] CMS Collaboration, Observation of new structure in the $J/\psi J/\psi$ mass spectrum in proton-proton collisions at $\sqrt{s} = 13$ TeV, [arXiv:2306.07164 [hep-ex]].
- [4] Belle Collaboration, Observation of a narrow charmonium-like state in exclusive $B^\pm \rightarrow K^\pm \pi^+ \pi^- J/\psi$ decays, Phys. Rev. Lett. **91** (2003), 262001 doi:10.1103/PhysRevLett.91.262001 [arXiv:hep-ex/0309032 [hep-ex]].
- [5] M. Pivk and F. R. Le Diberder, SPlot: A Statistical tool to unfold data distributions, Nucl. Instrum. Meth. A **555** (2005), 356-369 doi:10.1016/j.nima.2005.08.106 [arXiv:physics/0402083 [physics.data-an]].
- [6] LHCb Collaboration, Observation of structure in the J/ψ -pair mass spectrum, Sci. Bull. **65** (2020) no.23, 1983-1993 doi:10.1016/j.scib.2020.08.032 [arXiv:2006.16957 [hep-ex]].
- [7] ATLAS Collaboration, Observation of an excess of di-charmonium events in the four-muon final state with the ATLAS detector, [arXiv:2304.08962 [hep-ex]].